Kinetics of propyl acetate oxidation: Experiments in a jet-stirred reactor, ab initio calculations, and rate constant determination

Guillaume Dayma, Sébastien Thion, Maxence Lailliau, Zeynep Serinyel, Philippe Dagaut, Baptiste Sirjean, René Fournet

Kinetics of propyl acetate oxidation: experiments in a jet-stirred reactor, *ab initio* calculations, and rate constant determination

Guillaume Dayma[1,2]*, Sébastien Thion[1,2], Maxence Lailliau[1,2], Zeynep Serinyel[1,2], Philippe Dagaut[1], Baptiste Sirjean[3,4], and René Fournet[4]

[1] CNRS-INSIS, Institut de Combustion, Aérothermique, Réactivité et Environnement, 1C avenue de la recherche scientifique, 45071 Orléans cedex 2, France

[2] Université d'Orléans, 6 avenue du Parc Floral, 45100 Orléans, France

[3] CNRS-INSIS, Laboratoire de Réaction et Génie des Procédés, 1 rue Grandville, 54000 Nancy, France

[4] Université de Lorraine, 1 rue Grandville, 54000 Nancy, France

*Corresponding author:

Prof. Guillaume Dayma

CNRS-INSIS, Institut de Combustion, Aérothermique, Réactivité et Environnement

1C Avenue de la Recherche Scientifique - 45071 Orléans Cedex 2, France

Tel: +33 (0) 238 25 54 99 - Fax: +33 (0) 238 69 60 04 - guillaume.dayma@cnrs-orleans.fr

Colloquium: Gas-Phase Reaction

Total length of paper (method 1):	**6014 Words**
Main text:	3079 Words
References: (30+2) × (2.3 lines/reference) × 7.6 words/lines) =	559 Words
Figure 1: (33mm+10mm) × (2.2 words/mm) × 1 column + 28 words in caption =	123 Words
Figure 2: (42mm+10mm) × (2.2 words/mm) × 2 columns + 22 words in caption =	251 Words
Figure 3: (82mm+10mm) × (2.2 words/mm) × 1 columns + 31 words in caption =	233 Words
Figure 4: (57mm+10mm) × (2.2 words/mm) × 1 columns + 34 words in caption =	181 Words
Figure 5: full page (900) + 46 words in caption =	946 Words
Figure 6: (53mm+10mm) × (2.2 words/mm) × 1 column + 34 words in caption =	173 Words
Figure 7: (50mm+10mm) × (2.2 words/mm) × 1 column + 54 words in caption =	186 Words
Table 1: (4 lines + 2) × (7.6 words/line) × 2 column + 23 words in caption =	114 Words
Equation 1: (3 lines + 2) × (7.6 words/line) =	38 Words
Abstract:	**131 Words**

Submitted for consideration at the 37th International Symposium on Combustion, Dublin, 2018

Abstract

In this study, the oxidation of propyl actetate (PA) was investigated experimentally in a jet-stirred reactor and theoretically by electronic structure calculations. Experiments were performed at 1 and 10 atm for three different equivalence ratios (φ = 0.5, 1, and 2) at each pressure. These experimental results show the strong influence of the molecular reaction yielding propene and acetic acid throughout the investigated temperature range (700 – 1250 K). In order to better understand the oxidation process of propyl acetate, a detailed kinetic mechanism consisting of 628 species involved in 3927 reversible reactions has been developed laying on previous works on esters oxidation and theoretical calculations performed in this study. These calculations compare well with the rate constant experimentally determined in our jet-stirred reactor for the molecular reaction: $k = 1.292 \times 10^{13} exp\left(-\frac{25167}{T}\right)$ (s^{-1}) (700 – 1010 K).

Keywords: propyl acetate, kinetics, modeling, *ab initio* calculations, jet-stirred reactor

1. Introduction

This work reports the first oxidation study of propyl acetate at atmospheric and high pressure. Propyl esters have received little attention up to now. However, bio-propanol is a promising alcohol fuel that could be used in the transesterification process with vegetable oil, thus providing propyl esters, potential additives for biodiesel. To the best of our knowledge, previous studies on propyl acetate mostly focused on the molecular elimination of propene and acetic acid. In 1963, Scheer et al. [1] measured the rate constant of the molecular elimination of alkene and acetic acid for 27 aliphatic acetates in a micro-scale flow reactor over the temperature range 725 < T < 810 K. Later, de Burgh Norfolk and Taylor [2]

extended the temperature range towards lower temperatures and confirmed the previous evaluation. More recently, Tosta et al. [3] have used several DFT methods to perform kinetic calculations on the unimolecular gas-phase elimination of primary alkyl acetates including propyl acetate. However, the low levels of theory considered lead to rate constants around one to four orders of magnitude higher than those experimentally obtained earlier [1, 2].

The aim of this work is two-fold: (i) provide experimental data for propyl acetate kinetics of oxidation and (ii) propose and validate a new kinetic reaction scheme for PA oxidation. To this end, (i) detailed speciation data in the intermediate-to-high temperature range (700 – 1250 K) were obtained using a jet-stirred reactor, (ii) rate constants for key reactions were derived from theoretical calculations in order to generate an oxidation kinetic model for PA, and (iii) the proposed kinetic scheme was validated against the present data.

2. Experimental apparatus

The oxidation of propyl acetate was studied in a fused silica jet-stirred reactor (JSR) extensively described earlier [4, 5]. Three mixtures of different equivalence ratios (φ = 0. 5, 1.0 and 2.0) were considered with a constant initial fuel mole fraction of 1000 ppm (+/- 10%). This high dilution level prevents temperature gradients inside the reactor. Experiments were carried out at 1 and 10 atm and the reactants flow rates were adjusted at each temperature to reach a constant residence time of 70 ms and 700 ms, respectively. The liquid fuel (from Sigma Aldrich CAS 109-60-4 – purity ≥ 99%) was handled by a HPLC pump and sprayed by a nitrogen flow through a pin hole into a heated chamber. A quartz capillary led the fuel-nitrogen mixture to the entrance of the injectors, where it met the oxidizing mixture (N_2+O_2). Stirring was finally ensured by high turbulence produced by four nozzles and a steady state was quickly reached. The reactor was heated by two furnaces and the temperature was measured by a 0.1 mm Pt-Pt/Rh-10% thermocouple located inside a thin wall quartz tube.

Gases were sampled by a low-pressure sonic probe to freeze the chemical reactions. They were analyzed online by Fourier transform infrared spectroscopy or stored at low-pressure into Pyrex bulbs for off-line gas chromatography analyses. Carbon balance was checked for each experiment and found to be within 10%. The species measured were propyl acetate, O_2, H_2O, CO, CO_2, H_2, methane, ethylene, propene, 1-butene, 1,3-butadiene, acetylene, acrolein, acetic acid, acetaldehyde, and formaldehyde. The uncertainty on species mole fractions is estimated to be ca. 15% based on uncertainties on the analytical measurements, temperature measurements (less than 10 K), pressure measurements (± 0.1 atm), the residence time (less than 5%) and on inlet concentrations of the reactants (less than 10%).

3. Computational Methodology

Quantum chemistry calculations were used to compute the high-pressure rate coefficients of the pericyclic reaction involved in the formation of acetic acid and propene from propyl acetate. Geometry and frequency calculations were performed at the M06-2X/6-311++G(3df,2pd) level of theory from the GAUSSIAN 09 Rev. D01 software [6]. This density functional method, combined with a large basis set, allows a good estimation of both molecular geometries and harmonic frequencies [7]. A scaling factor of 0.983 was used to take into account anharmonicity, in accordance with reference [8]. The M06-2X method was also considered to perform the one-dimensional relaxed scans needed for the treatment of hindered rotors (see above), but a lower basis set was used in this latter case (6-311+G(d,p)). Electronic energy was computed at the CCSD(T) level of theory by means of the CCSD(T)-F12 method associated with theVTZ-F12 basis set, available in MOLPRO [9]. The high-pressure rate coefficients were computed from canonical transition state theory combined with statistical thermodynamics (see Supplementary Material). Internal rotations were treated as hindered rotors (HR) by means of a modified one-dimensional hindered rotor formalism (1-

DHR). In this approach, harmonic frequencies corresponding to HR are recalculated rather than being (arbitrarily) chosen among the list of frequencies given by the normal mode analysis. Thus, the partition function obtained can be expressed by the following relation:

$$Q_{1-DHR-U} = Q_{HO} \prod_{j=1}^{N} \frac{q_{1-DHR,j}}{q_{HO,j}} \quad (1)$$

where Q_{OH} is the full partition function in the harmonic oscillator approximation, $q_{1-DHR,j}$ is the partition function of the torsional mode *j*, computed in the 1-DHR approximation and $q_{OH,j}$ is the recalculated harmonic partition function for the same torsional mode but treated as a one-dimensional mode (pure 1D harmonic oscillator).This approach was also used to evaluate entropies and heat capacities of the reactants and products. All calculations were performed using the THERMROT software [10]. In addition, RRKM/master equation analysis was carried out by means of the kinetic code MESS [11] in order to investigate the pressure effect in our operating conditions. The interactions between propyl acetate and the bath gas (N_2) were modeled with the Lennard-Jones potential (see Supplementary Material). In order to find the lower energy conformer of propyl acetate (Figure 1), eighteen conformers were generated by considering the rotations around the C–C and C–O bonds by means of the "ConfGen" module implemented in the MSTor software [12]. Rotations around the methyl groups were not taken into account because they lead to indistinguishable conformers and only two rotations around the C_{10}–O_{12} bond were investigated (Figure 1), due to the planar structure formed by atoms C_{14}, C_{10}, O_{11} and O_{12}. The lower energy conformer found lies around 0.15 kcal mol^{-1} (zero point including energy) below the *all-trans* conformer.

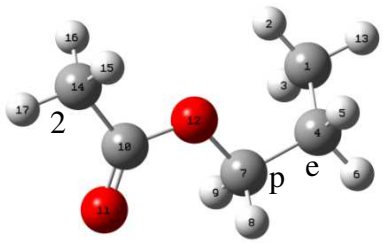

Figure 1. Lower energy conformer of propyl acetate ($C_5H_{10}O_2$) obtained at the M06-2X/6 311++G(3df,2pd) level of theory. Carbons “2”, “p”, “e”, and “m” refer to the mechanism nomenclature.

The standard entropy at 298 K and heat capacity of $C_5H_{10}O_2$ were computed using the THERMROT software [10], while its standard enthalpy of formation at 298 K was obtained from isodesmic reactions (see Supplementary Material). Table 1 summarizes the results obtained and gives comparisons with available experimental results. These results show a good agreement and validates the method chosen for the treatment of hindered rotations as the computed entropy is close to the experimental value (around 0.5%), whereas the purely harmonic treatment leads to a significantly lower value (91.41 cal mol^{-1} K^{-1}).

Table 1. Thermodynamic properties of propyl acetate. $\Delta_fH°_{298K}$ is given in kcal mol^{-1} while

$\Delta_fH°_{298K}$	$S°_{298K}$	$C_p°$					
		298 K	400 K	600 K	800 K	1000 K	1500 K
-110.3	95.65	30.64	38.86	52.16	62.21	69.62	80.38
-111.09 [13]	96.15 [13]		38.80 [14]				

$S°_{298K}$ and $C°_p$ are expressed in cal mol^{-1} K^{-1}.

4. Rate constant of the molecular reaction

4.1- Theoretical determination

The formation of acetic acid from propyl acetate involves a 6-membered cyclic transition state. Since, in our study, the ring puckering is not considered as a specific motion

but treated as harmonic vibration, two TS (with two optical isomers) must be considered, depending on the position of the methyl group with respect to the cycle (Figure 2).

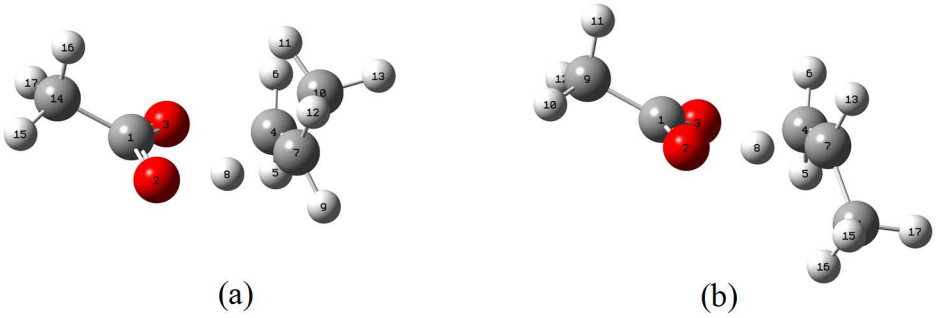

(a) (b)

Figure 2. Transition states involved in the formation of acetic acid from propyl acetate. Geometry obtained at the M06-2X/6-311++G(3df,2pd) level of theory.

Single point energy calculations performed, both for propyl acetate and the two TS, at the CCSD(T)-F12/VTZ-F12 level of theory, lead to energy barriers (zero point including energy) of 49.80 kcal mol^{-1} (TS_a) and 49.93 kcal mol^{-1} (TS_b). The high-pressure rate constant was computed in the temperature range [500–2000K] and fitted with the following modified Arrhenius relationship: $k_\infty = 5.88 \times 10^8 \ T^{1.299} exp\left(-\frac{23933}{T}\right) \ (s^{-1})$.

4.2- Experimental determination

Under our experimental conditions, it was observed that the conversion of propyl acetate was independent of the equivalence ratio at a given pressure as can be seen from Figure 3. This indicates that the reactivity is mostly driven by molecular reactions instead of reactions involving radicals since the radical pool is usually affected by the equivalence ratio. In addition, the only products that were significantly detected at temperatures below 1050 K at 1 atm were propene (Figure 3) and acetic acid. At 10 atm and φ = 1.0 and 2.0, propene accumulates up to nearly 1000 ppm whereas it is consumed at lower temperature at φ = 0.5 (ca. 860 K). This confirms the fact that the only molecular reaction involved in the

consumption of propyl acetate under these conditions is the concerted elimination of propene and acetic acid. This observation will be confirmed by the reaction pathways analysis performed using our chemical kinetic mechanism (section 6). It was thus possible to determine experimentally this rate constant using the mass balance equation of propyl acetate and propene in an open flow reactor and considering a first-order law for the consumption of propyl acetate: $X_{i,PA} - X_{e,PA} = k\tau X_{e,PA}$ in the case of PA and $X_{e,Prod} = k\tau X_{e,PA}$ in the case of C_3H_6 and CH_3COOH, where $X_{i,\ PA}$ is the initial PA mole fraction introduced in the JSR, $X_{e,PA}$, the PA mole fraction measured experimentally at the exhaust, $X_{e,Prod}$, either the propene or acetic acid mole fractions measured experimentally at the exhaust, τ, the residence time and k, the rate constant of the unimolecular reaction to be determined. The experimental rate constant can be represented in Arrhenius form as: $k = 1.292 \times 10^{13} exp\left(-\frac{25167}{T}\right)\ (s^{-1})$ (700 – 1010 K).

Figure 4 shows the comparison between our theoretical rate constant calculated as explained in section 4.1, the experimental values deduced from the measurements performed in our jet-stirred reactor, at different pressures and equivalence ratios and for temperatures ranging from 625 to 1100 K, and experimental data available in the literature [1, 2]. This figure shows a good agreement between theoretical calculations and experimental data. It is worth noting that the study performed by de Burgh Norfolk and Taylor [2] has been carried out at low pressure (P = 0.2 atm). Under the investigated pressure range (0.2 – 10 atm), this rate constant does not seem to have any pressure dependency. This observation was confirmed by RRKM/master equation analysis performed by means of the kinetic code MESS [11], for temperatures and pressures ranging, respectively, from 650 to 2000 K and 0.1 to 10 bar (see Supplementary Material).

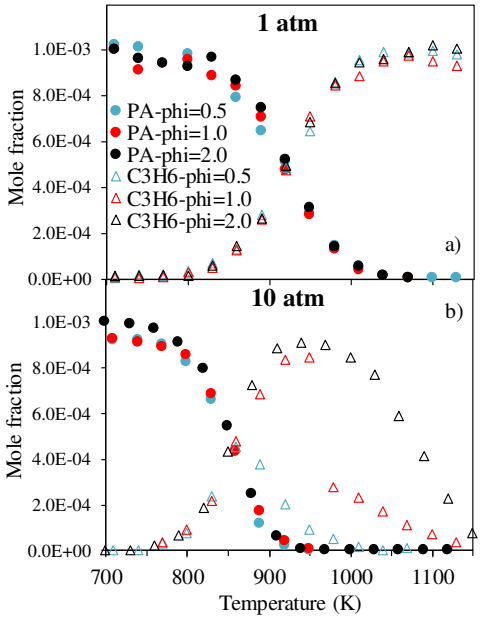

Figure 3. Experimental evolution of the mole fractions of propyl acetate and propene as a function of the temperature at a) 1 atm and b) 10 atm and different equivalence ratios.

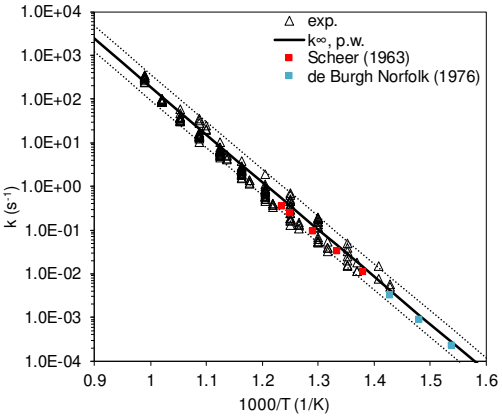

Figure 4. Comparison between theoretical calculations and experimental values for the rate constant involved in the formation of propene and acetic acid from propyl acetate (dotted lines denote an uncertainty factor of 2).

5. Modeling

The mechanism developed in this study is based on our previous works on esters oxidation [5, 15, 16]. Unimolecular initiations of PA by C–H and C–C bond breaking were taken from

[17]. H-abstractions by H atoms come from our recent works on butanone [18] for carbon "2", on butyl formate for carbons "p" and "e" [16], and the study by Sivaramakrishnan et al. [19] for carbon "m". For H-abstractions by OH and HO_2, rate constants were taken from Mendes et al. [20, 21]. H-abstractions by O and CH_3, isomerizations and β-scissions were also taken from our previous works [5, 22, 23]. Due to the abundant production of acetic acid during the oxidation of propyl acetate, a specific attention was paid to the development of a sub-mechanism for this organic acid. Initiation reactions by C–C and C–O bond breaking come from the work by Christensen and Konnov [24] as it is for H-abstractions by O and HO_2. The consumption of acetic acid under these conditions yield methane and CO_2 on one hand and ketene and water on the other. For both of these reactions, the rate constant was estimated from the rate constant proposed by Elwardany et al. [25] at high temperature and that proposed by Blake and Jackson [26] at low temperature. H-abstractions by H, OH, and CH_3 were taken from Mendes et al. [27]. The β-scission yielding ketene and OH from CH_2COOH was reevaluated from the work by Brown et al. [28] and the branching ratios calculated by Hou et al. [29]. This mechanism involving 628 species and 3927 reversible reactions was finally used to simulate the JSR experiments. These simulations were carried out with the Perfectly Stirred Reactor (PSR) code [30] of the Chemkin II package.

6. Experimental and modeling results

The mole fraction profiles obtained at different equivalence ratios at 10 atm are illustrated in Figure 5. As can be seen from this figure, fuel consumption starts ca. 760 K, regardless of the equivalence ratio. In the meantime, propene and acetic acid accumulate. Under fuel-lean conditions, up to 860 K, the carbon balance is ensured by only these three species. The same is observed for the stoichiometric mixture up to 920 K, and for the fuel-rich mixture up to 970 K. Whereas the consumption of propyl acetate is independent of equivalence ratio, those of

C_3H_6 and CH_3COOH are clearly related to the initial O_2 concentration. Moreover, for the stoichiometric mixture, the consumption of the products of the molecular reaction starts abruptly: between 960 and 970 K, the mole fraction of propene decreases by a factor of three, which is well captured by the mechanism. Conversely, the conversion of propene under fuel-rich conditions is gradual: the mole fraction of propene is divided by 3 over 150 K. However, a brutal consumption is also foreseen by the kinetic mechanism for the fuel-lean mixture, which is not clearly observed experimentally. Once the consumption of propene and acetic acid starts, it is accompanied by the formation of final products and intermediates. The formation of these intermediates is thus directly linked to the reactivity of both propene and acetic acid. For instance, the accumulation of methane and ethylene is shifted towards higher temperatures when the equivalence ratio increases as is the onset of the consumption of propene and acetic acid. Results obtained under atmospheric pressure, for which good agreement between experimental and modeling results was observed, are reported as Supplementary Material.

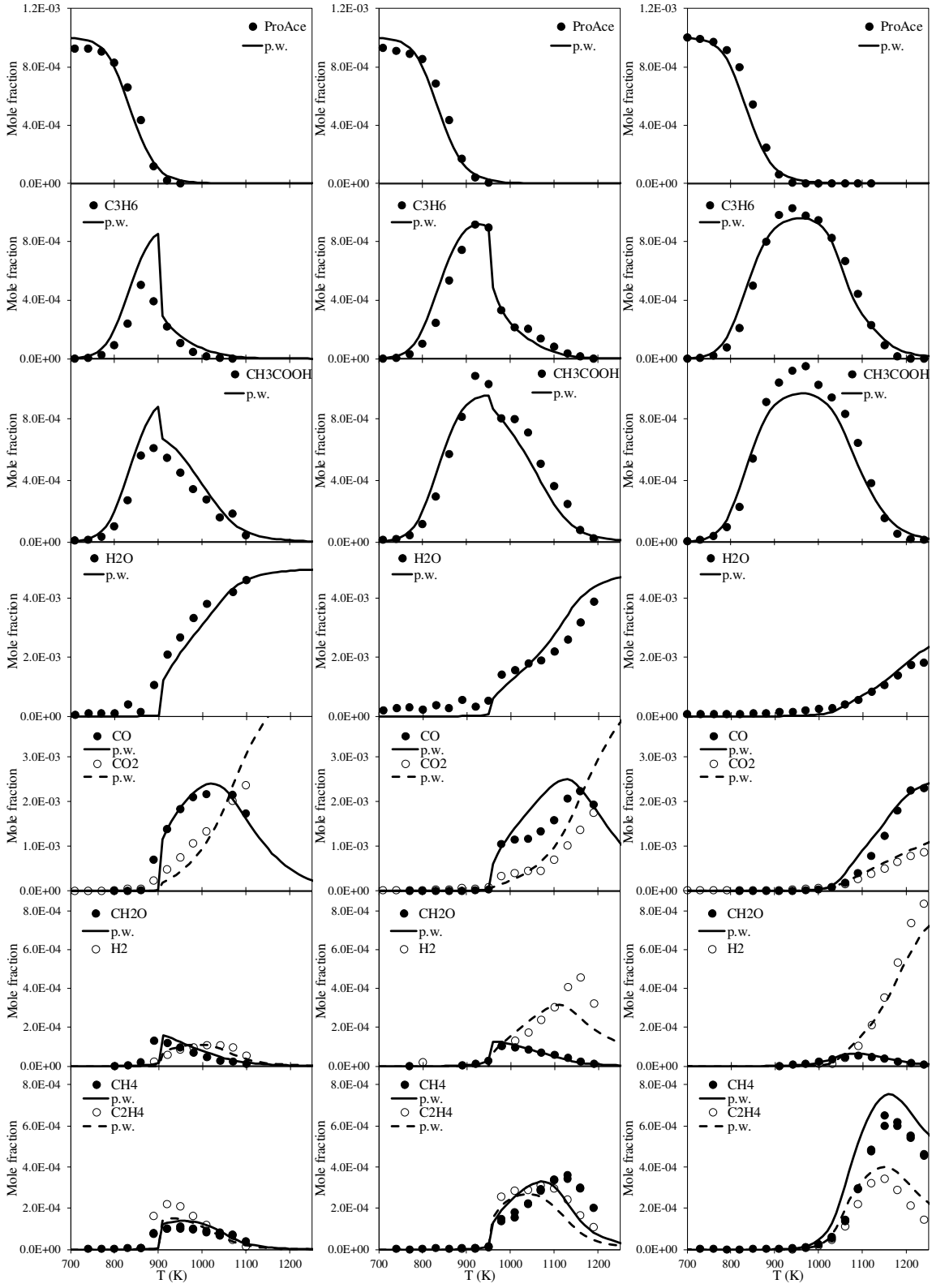

Figure 5. Experimental (symbols) and simulated (lines) mole fraction profiles obtained from the oxidation of propyl acetate in a JSR at φ = 0.5 (left), φ = 1.0 (center), and φ = 2.0 (right), X_{PA} = 1000 ppm, P = 10 atm, and τ = 0.7s.

Reaction pathways analysis

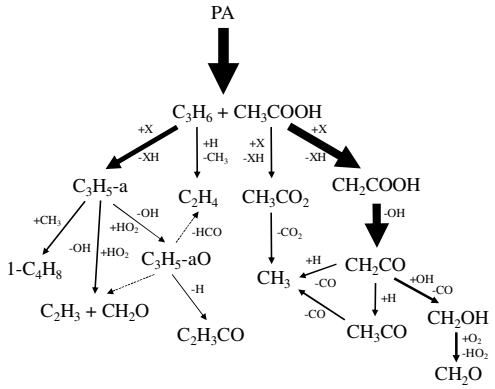

Figure 6. Normalized rates of reaction analysis at $\varphi = 1$, $\tau = 0.7$ s, P = 10 atm and T = 1000 K (*The thickness of the arrows is proportional to the flow rate).*

Figure 6 shows that the molecular reaction of the fuel yielding propene and acetic acid is the only consumption pathway. At temperature, below 970 K, C_3H_6 and CH_3COOH are not consumed under these conditions, but at 1000 K, the conversion of these products has started. Propene is mostly consumed by H-abstractions (OH: 32.6%, H: 4.2%, HO_2: 3.9%, CH_3: 2.1%) to give allyl radical. 17% of C_3H_6 reacts by ipso-addition with H atoms and gives C_2H_4 and CH_3. By H atom addition, propene can also produce to a smaller extent (14%) propyl isomers which in turn give back propene by oxidation by O_2 eliminating HO_2. The major consumption pathway of allyl radicals is the addition with CH_3 yielding 1-butene (34%). Allyl can also react with HO_2 eliminating OH to give either the vinyl radical and formaldehyde (31%) or the allyloxy radical (20%). Finally, the allyloxy radical decomposes into the vinyl radical and formaldehyde (13%) or acrolein (74%) eliminating an H atom. As for propene, acetic acid reacts almost exclusively by H-abstractions on the methyl group (72%) or on the acid group (15%). CH_2COOH then eliminates OH yielding ketene, while CH_3CO_2 decomposes into CH_3 and CO_2. Ketene appears as a key intermediate in the oxidation process of acetic acid but it was unfortunately not possible to measure it. Ketene mostly produce

methyl radicals (49%) by reaction with H atoms, either directly or through the formation of acetyl radicals. Ketene also reacts with OH (32%) eliminating CO and producing CH_2OH, which in turn yield formaldehyde by oxidation with O_2.

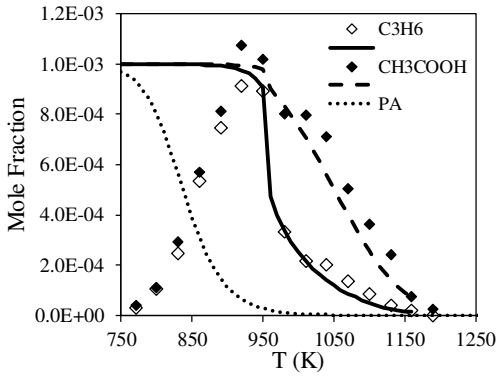

Figure 7. Comparison of the evolution of the experimental mole fractions of C_3H_6 and CH_3COOH measured at $\varphi = 1$, $\tau = 0.7$ s, P = 10 atm and $X_{PA} = 1000$ ppm with the computed mole fractions of a mixture of 1000 ppm of C_3H_6 and 1000 ppm of CH_3COOH under the same conditions.

Figure 7 presents a comparison of the evolution of the mole fractions of propene and acetic acid measured at $\varphi = 1$, $\tau = 0.7$ s, P = 10 atm and $X_{PA} = 1000$ ppm with the computed mole fractions of a mixture of 1000 ppm of C_3H_6 and 1000 ppm of CH_3COOH, the equivalence ratio, the residence time and the pressure being the same. As can be seen from this figure, when propyl acetate is consumed between 750 and 950 K, C_3H_6 and CH_3COOH accumulate without reacting up to a given temperature and their mole fractions reach ca. 1000 ppm (their maximum mole fraction). Above 950 K, their consumption starts and the experimental mole fraction of propene decreases as abruptly as in the case of the mixture of 1000 ppm of propene and 1000 ppm of acetic acid as initial fuels, and the computed and experimental profiles match almost perfectly. It clearly shows this system behaves in two steps: first, the decomposition of propyl acetate and the accumulation of propene and acetic acid, and second,

at higher temperature, the consumption of propene and acetic acid. Under this condition, there is virtually no overlap between both steps, allowing to determine the rate constant of the molecular decomposition of propyl acetate.

7. Conclusion

New experimental data were obtained for the oxidation of propyl acetate in a JSR at 1 and 10 atm, in the temperature range 700–1250 K, and for equivalence ratios of 0.5, 1.0, and 2.0. They consist of mole fraction profiles of the reactants, final products, and stable intermediates measured by gas chromatography, mass spectrometry, and Fourier transform infrared spectrometry after sonic probe sampling. A detailed kinetic model was proposed and tested against the experimental data obtained in this work. This model was developed based on previous kinetic schemes for the oxidation of other oxygenated fuels and on theoretical calculations at the CCSD(T)-F12/VTZ-F12//M06-2X/6-311++G(3df,2pd) level of theory for the molecular elimination of propene and acetic acid. This new model performs well against the available experimental data. Reaction pathways and sensitivity analyses were used to interpret the results. The study shows that for the fuel, consumption by molecular elimination is the most important reaction pathway whereas the formation of other intermediates and final products is driven by the conversion of propene and acetic acid. Ketene and the allyl radical were found to be key intermediates. More data would be needed, especially for ignition and burning velocities to assess the validity of their sub-mechanism and further validate the PA oxidation kinetic mechanism.

8. Supplementary Material

Experimental mole fractions measured in JSR at $\varphi = 0.5$, $\varphi = 1.0$, and $\varphi = 2.0$, $X_{PA} = 1000$ ppm, P = 1 atm, and $\tau = 0.07$s. Pressure-dependence investigation of the molecular

elimination of propene and acetic acid. A comparison of rate constants from the literature for the elimination of alkenes and acids. Nomenclature of the different species involved in the mechanism. Detailed mechanism and thermodynamic data in the Chemkin format, geometries of the different species at the M06-2X/6-311++G(3df,2pd) level of theory used for the calculations.

9. Acknowledgements

The research leading to these results has received funding from the European Research Council under the European Community's Seventh Framework Program (FP7/2007–2013)/ERC grant agreement No.291049–2G-CSafe. Financial support from the Labex Caprysses (convention ANR-11-LABX-0006-01) and MESRI (M.L. doctoral grant) are gratefully acknowledged. This work was granted access to the HPC resources of IDRIS under the allocation 2018-A0010807249 made by GENCI.

10. References

[1] J.C. Scheer, E.C. Kooyman, F.L.J. Sixma, Recueil des Travaux Chimiques des Pays-Bas 82 (11) (1963) 1123-1154.

[2] S. de Burgh Norfolk, R. Taylor, Journal of the Chemical Society, Perkin Transactions 2 (3) (1976) 280-285.

[3] M.M. Tosta, J.R. Mora, T. Cordova, G. Chuchani, Journal of Molecular Structure: THEOCHEM 952 (1) (2010) 46-55.

[4] P. Dagaut, M. Cathonnet, J.P. Rouan, R. Foulatier, A. Quilgars, J.C. Boettner, F. Gaillard, H. James, Journal of Physics E: Scientific Instruments 19 (3) (2000) 207-209.

[5] G. Dayma, F. Halter, F. Foucher, C. Togbé, C. Mounaim-Rousselle, P. Dagaut, Energy & Fuels 26 (8) (2012) 4735-4748.

[6] M.J. Frisch, G.W. Trucks, H.B. Schlegel, G.E. Scuseria, M.A. Robb, J.R. Cheeseman, G. Scalmani, V. Barone, B. Mennucci, G.A. Petersson, et al., Gaussian 09, Revision D.01, Wallingford CT (2009).

[7] Y. Zhao, D.G. Truhlar, Theor Chem Account 120 (1) (2008) 215-241.

[8] I.M. Alecu, J. Zheng, Y. Zhao, D.G. Truhlar, Journal of Chemical Theory and Computation 6 (9) 2872-2887.

[9] H.J. Werner, P.J. Knowles, G. Knizia, F.R. Manby, M. Schütz, and others, Wiley Interdisciplinary Reviews: Computational Molecular Science 2 (2) (2012) 242-253.

[10] J.C. Lizardo-Huerta, B. Sirjean, R. Bounaceur, R. Fournet, Physical Chemistry Chemical Physics 18 (17) (2016) 12231-51.

[11] Y. Georgievskii, J.A. Miller, M.P. Burke, S.J. Klippenstein, J. Phys. Chem. A 117 (46) 12146-12154.

[12] J. Zheng, R. Meana-Pañeda, D.G. Truhlar, Computer Physics Communications 184 (8) (2013) 2032-2033.

[13] R. Rowley, W. Wilding, J. Oscarson, Y. Yang, N. Zundel, T. Daubert, R. Danner, Design Institute for Physical Properties (2006).

[14] J.E. Connett, J.F. Counsell, D.A. Lee, The Journal of Chemical Thermodynamics 8 (12) (1976) 1199-1203.

[15] G. Dayma, S.M. Sarathy, C. Togbé, C. Yeung, M.J. Thomson, P. Dagaut, Proceedings of the Combustion Institute 33 (1) (2011) 1037-1043.

[16] A.M. Zaras, M. Szőri, S. Thion, P. Van Cauwenberghe, F. Deguillaume, Z. Serinyel, G. Dayma, P. Dagaut, Energy & Fuels 31 (6) (2017) 6194-6205.

[17] G. Dayma, F. Halter, F. Foucher, C. Mounaim-Rousselle, P. Dagaut, Energy & Fuels 26 (11) (2012) 6669-6677.

[18] S. Thion, P. Diévart, P. Van Cauwenberghe, G. Dayma, Z. Serinyel, P. Dagaut, Proceedings of the Combustion Institute.

[19] R. Sivaramakrishnan, J.V. Michael, B. Ruscic, International Journal of Chemical Kinetics 44 (3) (2012) 194-205.

[20] J. Mendes, C.-W. Zhou, H.J. Curran, The Journal of Physical Chemistry A 118 (27) (2014) 4889-4899.

[21] J. Mendes, C.-W. Zhou, H.J. Curran, The Journal of Physical Chemistry A 117 (51) (2013) 14006-14018.

[22] G. Dayma, S. Gaïl, P. Dagaut, Energy and Fuels 22 (3) (2008) 1469-1479.

[23] G. Dayma, C. Togbé, P. Dagaut, C. Togbé, P. Dagaut, C. Togbé, P. Dagaut, Energy & Fuels 23 (9) (2009) 4254-4268.

[24] M. Christensen, A.A. Konnov, Combustion and Flame 170 (2016) 12-29.

[25] A. Elwardany, E.F. Nasir, E. Es-sebbar, A. Farooq, Proceedings of the Combustion Institute 35 (1) (2015) 429-436.
[26] P.G. Blake, G.E. Jackson, Journal of the Chemical Society B: Physical Organic (0) (1969) 94-96.
[27] J. Mendes, C.-W. Zhou, H.J. Curran, The Journal of Physical Chemistry A 118 (51) (2014) 12089-12104.
[28] A.C. Brown, C.E. Canosa-Mas, A.D. Parr, R.P. Wayne, Chemical Physics Letters 161 (6) (1989) 491-496.
[29] H. Hou, B. Wang, Y. Gu, Physical Chemistry Chemical Physics 2 (10) (2000) 2329-2334.
[30] P. Glarborg, R.J. Kee, J.F. Grcar, J.A. Miller, PSR: A Fortran Program for Modeling Well-Stirred Reactors, Sandia National Laboratories, Albequerque, NM, 1986.

11. List of figures